Analysis of foot skeletal structure by 3D foot scanner on smartphone

Tomoko Yamashita (d19tb552@eb.osaka-cu.ac.jp)
Osaka University https://orcid.org/0000-0003-4914-0306
Kazuhiko Yamashita
Ryotokuji University
Mitsuru Sato
Showa University
Takeshi Ryotokuji
Ryotokuji University
Masashi Kawasumi
Tokyo Denki University
Yoshimasa Takase
Takase Clinic
Shinsuke Hara
Osaka City University

Research

Keywords: foot 3D scanner, smartphone, hallux valgus

Posted Date: September 10th, 2020

DOI: https://doi.org/10.21203/rs.3.rs-54805/v2

Abstract

Background: The influence of foot skeletal structure on hallux valgus (HV) is poorly understood, so its detailed understanding at an early stage is required for prevention. In this study, a system using a 3D foot scanner on smartphone was developed for the purpose of clarifying relationships between skeletal features and the degree of HV risk.

Methods: This system analyzes the foot skeletal structure by sending 2D video images recorded on smartphone to a computer or cloud server, where the 3D foot skeleton model is constructed by the 2D images. This system was developed to identify 10 skeletal features that are expected to be associated with hallux valgus. The participants comprised 419 individuals (40–89 years), and they maintained a standing pose with their toes 12 cm apart and heels 8 cm apart during the video recording. The height and weight were additionally measured to calculate BMI.

Results: The study results showed that age-based variations in the foot skeletal features were observed slightly for men whereas distinctively for women. It was observed for women that the great toe-first metatarsal head-heel (GFH) angle increases with age, so it suggests that the increase of the GFH angle characterizes the development of HV. The multiple regression analysis reveals that the features determining the GFH angle are the second toe-heel-navicular angle and the axis of the bone distance among the skeletal features related to the midfoot, and the transverse arch length and height among those related to the forefoot. Their adjusted coefficients of determination were 0.52 and 0.48 for men and women, respectively.

Conclusion: Using a 3D foot scanner on smartphone, we developed a simple method to access the skeletal structure of the foot related to HV risk.

Trial registration: University hospital Medical Information Network- Clinical Trials (UMIN-CTR) with the number: UMIN 000037694. Registration date: 20/08/2019.

Background

Hallux valgus (HV) is a common deformity characterized by abnormal angulation, rotation and lateral deviation of the great toe at the first metatarsophalangeal joint, and it occurs widely across all age groups. The prevalence for HV is 23% in adults aged 18–65 years and 35.7% in elderly people older than 65 years[1], and it is also higher for women than for men (30% vs. 13%)[1].

It has been reported that assessing the skeletal features of the foot is effective for examining HV[2]. Several factors have been reported to be associated with HV, such as gender[1,3], age[1], BMI[2], first metatarsal length[4,5], flatfoot[6], osteoarthritis[7,8] and footwear[9]. However, the degree to which foot skeletal influences HV is poorly understood[10]. As HV is highly prevalent, understanding the skeletal features of the foot at an early stage is required for prevention of HV. Quantitative analysis of foot shape is important for not only clinical assessment of foot deformities[11] but also a number of applications related to the ergonomic design of footwear, foot orthotics, insoles and so on.

There are mainly two methods for assessing the skeletal features of the foot region: laser 3D surface scanners and X-ray. Laser 3D surface scanners are expensive but they are often used to create custom-made shoes that are perfectly matched to the shape of the foot[11,12]. They have been used to assess aspects of foot shape such as length and circumference, but no prior study has examined their use for analyzing the skeletal features of the foot. On the other hand, X-ray is invasive and can be used only in medical institutions. In principle, as it produces a 2D image, there is room for error in measurement because of the photography angle, and furthermore the assessment process is dependent on the doctor's subjectivity. Nix et al. noted that HV is not adequately defined using X-ray, and there is no attempt to adjust for significant differences between groups[13].

Therefore, in this study, a simple 3D foot scanner system was implemented by a smart phone and a remote computer. The aim of this study was to clarifying the skeletal features of the foot measured for men and women in different age groups. We suggest that some of them can be preventive indexes for the risk of HV.

Methods

Development of a Foot Morphology 3D Scanner on Smartphone

In this study, a 3D scanner system that can analyze the skeletal features of an individual's own foot was developed. The key characteristic of this system is that its main hardware is a smartphone. As smartphones are now widely used devices, many people will be able to use this system using the devices' built-in cameras.

This system analyzes the skeletal features of the foot by sending 2D video images recorded on the smartphone to a computer or cloud server. Thus, the system does not require particularly high specifications. The video images can be recorded manually as long as the frame does not leave the foot during the recording. The spatial resolution of this system is 0.5 mm in an optimal environment, and the reproducibility is high[14].

The features of the foot region assessed in this study were the tip of the hallux, tip of the second toe, inside of the first metatarsal head, navicular bone, protruding part of the calcaneus, outside of the fifth metatarsal head, and talus head, all of which can be automatically detected by this system. To confirm that the system can correctly detect these skeletal features, they were also identified via palpation by a physical therapist who understands the skeletal construction of the foot. Good agreement was confirmed in both results, so it can be considered that the developed method properly grasps the skeletal features.

Figures 1 (a)-(d) show the definitions of foot skeletal features assessed in this study. The instep height (IH) is the distance between the sole and the talus head at the highest point of the instep; the navicular height (NH) is the distance between the sole and the navicular bone; and the instep (IS) angle is the angle formed among the tip of the hallux, the talus head and the heel (see Fig. 1 (a)). The second toe-heel-navicular (SHN) angle is the angle formed among the tip of the second toe, the navicular bone and the heel (see Fig. 1 (b)). The transverse arch length (TAL) is the distance between the inside of the first metatarsal head and the outside of the fifth metatarsal; the transverse arch height (TAH) is the maximal distance between the sole and the line touching the upper surface of the forefoot giving the TAL (see Fig. 1 (c)). The metatarsophalangeal heel (MPH) angle is the angle formed among the inside of the first metatarsal head, the heel and the outside of the fifth metatarsal head; the great toe-first metatarsal head-heel (GFH) angle is the angle formed among the tip of the hallux, the inside of the first metatarsal head and the heel; and the axis of the bone distance (ABD) is the distance from the center line between the heel and the tip of the second toe when the coordinate point of the talus head is projected to the floor (see Fig. 1 (d)). In addition to these, to determine the influence of toe length, the great toe-second toe ratio (GSR) is measured, which is the ratio of the distance between the tip of the second toe and the heel to the one between the tip of the hallux and the heel. Consequently, the 10 aforementioned features are calculated by a 3D foot scanner, however, these distance-based features are influenced by the foot length, in other words, the size of each parameter varies depending on the size of the foot. Therefore, they were standardized by dividing each by the distance between the heel and the hallux (the length of the foot) and multiplying by 100. In addition, to assess the influence of personal physique, the height and weight for each individual participant were also measured to calculate BMI.

From the above definitions of the foot skeletal features, it can be understood that the IH is an index measuring the transverse arch, the SHN angle is an indicator of pronated feet, TAL and TAH are indices of the lateral arch, the GFH angle is an indicator of HV, and the ABD indicates the point at which the skeleton is out of alignment. Note that the HV angle, which is defined as the angle between the longitudinal axis of the first metatarsal and that of the proximal phalanx [15], is clinically used to grade the severity of HV, such as Mild: 15–20°, Moderate: 21–39° and Severe: ≥ 40° [15]. In this study, much attention is paid to the GFH angle as a substitute for the HV angle that can be measured only by x-ray. Furthermore, if the skeletal features of the foot related to the GFH angle can be clarified, a preventive method can be proposed. Finally, Table 1 summarizes the 10 skeletal features.

TABLE 1 THE DEFINITIONS OF FOOT SKELETAL FEATURES

Abbreviation	Meaning	Definition
IH	Instep height	Distance between the sole and the talus head at the highest point of the instep
NH	Navicular height	Distance between the sole and the navicular bone
IS	Instep angle	Angle formed among the tip of the hallux, the talus head and the heel
SHN angle	Second toe-heel-navicular angle	Angle formed among the tip of the second toe, the navicular bone and the heel
TAL	Transverse arch length	Distance between the inside of the first metatarsal head and the outside of the fifth metatarsal
TAH	Transverse arch height	Maximal distance between the sole and the line on the metatarsals giving the TAL
MPH angle	Metatarsophalangeal heel angle	Angle formed among the inside of the first metatarsal head, the heel and the outside of the fifth metatarsal head
GFH angle	Great toe-first metatarsal head-heel angle	Angle formed among the tip of the hallux, the inside of the first metatarsal head and the heel
ABD	Axis of the bone distance	Distance from the center line between the heel and the tip of the second toe when the coordinate point of the talus head is projected to the floor
GSR	Great toe-second toe ratio	Ratio of the distance between the tip of the second toe and the heel to the one between the tip of the hallux and the heel

Subjects

Subjects were recruited through advertisements published through the public relations department of a city. All subjects, who were capable of walking without assistance, signed a consent form prior to participation, where the study design had been approved by the Ethical Review Board in Ryotokuji University (Authorization number: 1909).

The target group was consisted of 419 people (age range, 40–89; mean age, 62.8 ± 12.4 years), including 151 men (mean age, 65.6 ± 11.0 years) and 268 women (mean age, 63.8 ± 12.4 years). The gender and age of the participants are shown in Table 2. The inclusion criterion was an age of 40–90 years, whereas the exclusion criteria were as follows: lower limb musculoskeletal disorders; inability to walk independently; concomitant systemic diseases; clinical signs of joint laxity; and major lower limb trauma.

Measurement Methods

The measurements were taken using a commercially available smartphone (iPhone 6). The participants maintained a standing pose with their toes 12 cm apart and their heels 8 cm apart during the measurement. An individual measurer held the smartphone and recorded an approximately 12-sec video images panning each subject’s feet. The features of the subject’s feet identified by a physical therapist’s palpation were noted by sticking on a 4-mm diameter marker.

Note that as the measurements were similar between the left and right feet, the 3D foot skeletal model only on the right foot images were constructed.

TABLE 2 SUBJECT CHARACTERISTICS

		Number of subjects	Age	Height (m)	Weight (kg)	BMI
Men	Total	151	65.6 ± 11.0	1.669 ± 0.058	67.1 ± 10.2	24.0 ± 3.2
	40–64 years	50	52.5 ± 7.4	1.700 ± 0.054	72.4 ± 11.1	25.1 ± 3.9
	65–74 years	70	69.1 ± 2.9	1.667 ± 0.055	65.2 ± 9.2	23.4 ± 2.8
	>75 years	31	78.6 ± 3.7	1.625 ± 0.039	62.8 ± 7.2	23.8 ± 2.6
Women	Total	268	62.8 ± 12.4	1.544 ± 0.060	55.0 ± 9.4	23.1 ± 3.7
	40–64 years	120	51.2 ± 8.1	1.572 ± 0.053	57.6 ± 10.2	23.3 ± 4.1
	65–74 years	103	69.4 ± 2.6	1.533 ± 0.044	54.1 ± 8.2	23.1 ± 3.5
	>75 years	45	78.7 ± 3.1	1.493 ± 0.069	50.1 ± 7.3	22.5 ± 3.1

Data are presented as the mean ± SD

Statistics Analysis

SPSS version 24 was used for statistical analysis on the measured data. In the analysis, comparisons of the skeletal feature means were performed using Student's t-test for unpaired data; statistically significant differences between the feature means were assessed using one-way ANOVA with Tukey's post hoc test; relationships among the features were explored using Pearson's correlation coefficient; In the analysis, the GFH angle is considered as the approximate value of the hallux valgus angle. Therefore, multiple linear regression was used to find features strongly associated with the GFH angle; and the p-value of 0.05 was considered statistically significant.

Results

Measurements of Features

Table 3 shows the measurements obtained using the 3D foot scanner by gender. For men, no variation among age groups was observed for any features excluding GSR. For women, on the other hand, variations among age groups were observed for the NH, IS angle, MPH angle, TAL, TAH and GFH angle.

TABLE 3 THE RESULTS OF 3D FOOT SCANNER

	Total	40–64 years	65–74 years	>75 years	F value, p value
IH	29.2 ± 2.5	29.4 ± 2.6	28.8 ± 2.3	29.5 ± 2.9	p = 0.39
NH	19.5 ± 2.4	19.5 ± 2.4	19.5 ± 2.3	19.6 ± 2.6	p = 0.98
IS angle [degrees]	133.4 ± 5.9	133.2 ± 5.6	133.5 ± 6.1	133.5 ± 6.1	p = 0.97
MPH angle [degrees]	33.0 ± 1.7	32.6 ± 1.8	33.1 ± 1.8	33.1 ± 1.4	p = 0.12
TAL	41.2 ± 2.0	40.8 ± 2.0	41.4 ± 2.1	41.5 ± 1.7	p = 0.22
TAH	16.2 ± 1.3	16.1 ± 1.4	16.1 ± 1.1	16.5 ± 1.5	p = 0.26
GFH angle [degrees]	33.0 ± 6.1	32.6 ± 5.6	33.5 ± 6.0	32.6 ± 7.2	p = 0.65
SHN angle [degrees]	22.2 ± 3.0	22.5 ± 3.2	22.0 ± 2.9	22.3 ± 3.1	p = 0.64
ABD	4.18 ± 2.53	4.37 ± 2.57	3.99 ± 2.45	4.31 ± 2.67	p = 0.69
GSR	0.99 ± 0.02	1.00 ± 0.02	0.99 ± 0.02	0.99 ± 0.02	F(2,148) = 4.21, p <0.02
BMI	24.0 ± 3.2	25.1 ± 3.9	23.4 ± 2.8	23.8 ± 2.6	F(2,147) = 4.11, p <0.02

MEASUREMENTS

Men

Women

	Total	40–64 years	65–74 years	>75 years	F value, p value
IH	28.3 ± 2.5	28.4 ± 2.5	28.3 ± 2.5	27.6 ± 2.6	p = 0.17
NH	18.0 ± 2.6	18.2 ± 2.4	18.3 ± 2.5	16.9 ± 3.0	F(2,265) = 4.76, p <0.009
IS angle [degrees]	136.1 ± 5.8	135.3 ± 5.4	135.8 ± 6.1	139.0 ± 5.6	F(2,265) = 7.08, p <0.001
MPH angle [degrees]	33.6 ± 2.1	33.2 ± 2.0	33.9 ± 2.3	34.2 ± 1.6	F(2,265) = 5.82, p <0.001
TAL	42.0 ± 2.5	41.4 ± 2.3	42.3 ± 2.7	42.7 ± 2.0	F(2,265) = 5.81, p <0.003
TAH	15.9 ± 1.4	16.0 ± 1.5	16.0 ± 1.3	15.3 ± 1.3	F(2,265) = 4.48, p <0.01
GFH angle [degrees]	35.9 ± 6.6	34.5 ± 5.5	36.1 ± 6.8	39.3 ± 7.4	F(2,265) = 9.25, p <0.001
SHN angle [degrees]	23.3 ± 3.4	23.1 ± 3.4	23.3 ± 3.4	23.6 ± 3.3	p = 0.98
ABD	4.47 ± 3.05	4.46 ± 2.79	4.43 ± 3.25	4.61 ± 3.31	p = 0.95
GSR	0.99 ± 0.02	0.99 ± 0.02	0.99 ± 0.02	0.99 ± 0.02	p = 0.80
BMI	23.1 ± 3.7	23.3 ± 4.1	23.1 ± 3.5	23.1 ± 3.7	p = 0.40

The data are presented as the mean ± SD

TABLE 4

CORRELATIONS AMONG FOOT FEATURES

		1	2	3	4	5	6	7	8	9	10	11
1	GFH angle	1										
2	ABD	0.342**	1									
3	SHN angle	0.555**	0.489**	1								
4	IH	−0.234**	−0.329**	−0.13	1							
5	NH	−0.304**	−0.391**	−0.304**	0.654**	1						
6	IS angle	0.196*	0.095	0.201*	−.736**	−0.478**	1					
7	MPH angle	0.370**	−0.07	0.125	0.114	0.006	0.013	1				
8	TAL	0.462**	−0.05	0.161*	0.102	−0.02	0.03	0.942**	1			
9	TAH	−0.15	−0.13	−0.07	0.519**	0.423**	−0.372**	0.344**	0.267**	1		
10	GSR	0.008	0.037	−0.04	0.037	−0.1	0.066	-0.12	−0.1	−0.13	1	
11	BMI	0.109	−0.01	0.023	0.005	0.064	0.065	0.071	0.122	0.342**	−0.180*	1

Men

		1	2	3	4	5	6	7	8	9	10	11
1	GFH angle	1										
2	ABD	0.261**	1									
3	SHN angle	0.507**	0.404**	1								
4	IH	−0.038	−0.338**	−0.024	1							
5	NH	−0.174**	−0.343**	−0.216**	0.487**	1						
6	IS angle	0.153*	0.037	0.098	−0.657**	−0.339**	1					
7	MPH angle	0.379**	−0.055	0.185**	0.192**	0.037	0.124*	1				
8	TAL	0.508**	−0.052	0.213**	0.202**	0.022	0.114	0.953**	1			
9	TAH	−0.146*	−0.115	−0.044	0.377**	0.396**	−0.247**	0.304**	0.220**	1		
10	GSR	0.185**	−0.04	−0.077	−0.054	−0.117	0.223**	0.031	0.11	−0.021	1	
11	BMI	−0.003	−0.022	0.026	0.065	0.068	−0.021	0.164**	0.176**	0.461**	0.008	1

Women

Correlations among Features

Table 4 shows the correlation coefficients among the foot skeletal features measured by the 3D foot scanner. The GFH angle was correlated with the SHN angle, ABD, IS angle, MPH angle, TAL, TAH, and NH, respectively, for both men and women, and additionally with the IH for men. For both men and women, on the other hand, the ABD was correlated with the SHN angle, IH, and NH, respectively, the NH was correlated with the TAH and IS angle, respectively, the IS angle was correlated with the TAH, the MPH angle was correlated with TAL and TAH, respectively, and the TAL was correlated with the TAH. For both men and women, furthermore, the BMI was correlated with the TAH.

Multiple Regression Analysis for the GFH Angle

Table 5 shows five independent skeletal features related to the GFH angle for men and women, respectively. Four of them, which are common for men and women, comprise the SHN angle, TAL, TAH and ABD, and the remaining one is the BMI for men whereas the GSR for women. Concerning the strength of relationship, the regulated r2 was 0.52 for men whereas 0.51 for women. For both men and women, it was implicated that the skeletal features related to the forefoot and skeletal misalignment of the midfoot characterize the GFH angle.

TABLE 5 RESULTS OF MULTIPLE REGRESSION ANALYSIS CONCERNING THE GFH ANGLE

Variable	B	SE B	β	p value	r^2	Adjusted r^2
SHN angle	0.77	0.136	0.381	<0.001	0.536	0.52
TAL	143.02	18.558	0.467	<0.001	F for change in r^2	p value
TAH	−135.65	30.505	−0.28	<0.001	33.228	<0.001
BMI	0.26	0.114	0.14	0.02		
ABD	33.58	15.961	0.139	0.04		

Men

Variable	B	SE B	β	p value	r^2	Adjusted r^2
SHN angle	0.72	0.10	0.37	<0.001	0.52	0.51
TAL	1.24	0.12	0.47	<0.001	F for change in r^2	p value
TAH	−1.01	0.21	−0.22	<0.001	55.47	<0.001
ABD	0.26	0.10	0.12	0.01		
GSR	65.325	17.632	0.162	<0.001		

Women

Discussion

Measurements of Features

In the measurement results, age-based variations in the foot features were observed slightly for men whereas distinctively for women. Particularly, it is surmised for women that the lower NH and increasing flatness of the foot were related to aging. However, aging did not have a great impact on the SHN angle and ABD. The longitudinal arch of the foot is likely to be connected with the tibialis posterior muscle, the muscle strength in the sole and the transformations in the skeletal structure [16,17]. For these reasons, it is surmised that the lowering of the longitudinal arch is caused by severe declines in muscle function such as impairment of the tibialis posterior muscle[18], protrusion of the calcaneus[19] and pronation of the navicular bone[20] as well as the aging process. It is also surmised that the IS angle increases as the thickness of foot skeletal structure decreases with ages.

Correlations among Foot Features

The correlation coefficient between the MPH angle and the TAL is greater than 0.94 in Table 4 for both men and women, indicating a strong correlation, on the other hand, the TAL increases whereas the TAH decreases with age for women in Table 3. Taking into consideration that the MPH angle and TAL are skeletal features related to the width of the forefoot and the TAH is a skeletal feature related to the height of the forefoot, it is surmised that flattening of the forefoot is associated with a broad foot. Particularly, it is surmised for women that the GFH angle increases with age, which indicates the development of HV.

Paying attention to the GFH angle, the skeletal features identified as being correlated with it include the SHN angle and ABD, which are those related to the midfoot. As the SHN angle increases, which means that the navicular bone sticks out more, the ABD also increases with the inside of the midfoot deviating more inward. Therefore, this suggests that foot pronation is associated with the increase of the GFH angle thus HV. This suggestion is supported by the result of a prior study[21] that the risk of HV is significantly increased in persons with pronated foot function.

In addition, it was found that the ABD is correlated with the SNH angle ($r2 > 0.40$), IH (which denotes the health of the foot's skeletal structure) ($r2 > 0.33$) and NH (which denotes the height of the longitudinal arch) ($r2 > 0.34$) in Table 4. This suggests that misalignment of the skeletal structure of the midfoot is related to the health of feet, particularly, the formation of navicular and cuneiform bones. This misalignment is considered to be influenced by both early childhood development and aging process[22].

Furthermore, correlation between the IH and the TAH was observed for both men ($r2 = 0.52$) and women ($r2 = 0.38$) in Table 4. The reason why the correlation is lower for women could be that the transverse arch reflected by the TAH is more strongly influenced by footwear for women.

Finally, as for flatfeet which means the fall of the longitudinal arch, many discussions have utilized footprints[23,24]. From the viewpoint of biomechanics, the main cause of flatfeet may be the influence of the tibialis posterior muscle or the muscles in the sole[25]. Considering pronation, the navicular bone moves directly below these muscles while causing 3D changes in various directions, such as supination of the subtalar joint, pronation of the navicular bone and supination of the forefoot. Therefore, assessing the 3D skeletal structure of the foot is effective for pronation, which is the very benefit of the proposed system.

Multiple Regression Analysis for the GFH Angle

It was revealed from Table 5 that dominant skeletal features determining the GFH angle are the SHN angle and the ABD among those related to the midfoot whereas the TAL and the TAH among those related to the forefoot for both men and women. In addition to these features, it was revealed that one of the dominant features is the BMI for men whereas GSR for women. Regarding the multiple regression analysis, the adjusted coefficient of determination was 0.52 for men versus 0.48 for women, multicollinearity was confirmed in relation to none of the independent features, and β was large for both men and women in the SHN angle and the TAL.

As for other features associated with HV, prior studies pointed out lower BMI and high heel use for women aged 20–64 whereas higher BMI and flat feet for men[2,13]. Our results suggest that the etiologic mechanisms of HV may differ between men and women. Namely, although this study included neither extremely overweight nor underweight participants, it found an association of BMI with HV for men, which was not strong as compared to that in the prior study[2].

Overall Results

A prior study showed that the protrusion of the first metatarsal and the lengths of the first metatarsal and the proximal phalanx of the hallux were increased in both men and women with HV as compared to those in the control group[4], in other words, the first toe is a key part related to HV. On the other hand, this study showed that a longer second toe was associated with a larger GFH angle, in other words, the second toe was a key part related to HV. The reason of this difference may be that the length of the first metatarsal was compared with that of the second metatarsal in the prior study whereas the distance between the tip of the first toe and the heel was compared with that between the tip of the second toe and the heel in this study. The proximal phalanx of the hallux deviates laterally towards the second toe as HV develops, so the distance between the tip of the hallux and the heel gets shortened, naturally resulting in the appearance of longer second toe.

In this study, it has been highlighted that the GFH angle as an index of HV is influenced by the flatness of the forefoot and misalignment of the skeletal structure of the midfoot. In a prior study, the NH was used as an index of flatfeet, which was considered to influence HV[26]. In this study, on the other hand, the independent variable derived from the multiple regression analysis was not the NH but the SHN angle. As the SHN angle and NH were inversely correlated (-0.3– -0.2), it is quite natural that both height and position of the navicular bone can be key features for HV. The SHN angle is not on a horizontal plane, so simple 2D measurement systems cannot calculate it. On the other hand, the developed 3D scanner system can easily calculate the NH as well as the SHN angle, using an automatically constructed 3D foot skeleton model.

By using a 3D foot scanner on smartphone, we have been able to implement a simple quantitative method for assessing the skeletal structure of the foot. This will allow us to clarify the risk of HV.

LIMITATION

This study has several limitations. The measurement is performed from the outside of the foot, so there may be some errors between the GFH angle and the HV angle measured by x-ray. In addition, the measurement is performed manually, so handshake may introduce some errors in the measurement data. Furthermore, the 3D foot skeleton model is constructed by 2D images, so some errors may occur in the construction process.

Conclusions

In this study, a 3D foot scanning method using a smartphone was developed, and the skeletal structure of the foot was analyzed. One of the main results is that dominant skeletal features for determining the HV-related GFH angle are the SHN angle and ABD among those related to the midfoot whereas the TAH and TAL among those related to the forefoot. Another is that age-based variations in the foot skeletal features were observed slightly for men whereas distinctively for women.

Using a smartphone, it is possible to conduct a simple non-invasive assessment of the skeletal structure of the foot at any location. This will facilitate clarification of the factors of skeletal structure contributing to HV, and it is expected to improve efforts to prevent HV.

Abbreviations

HV: hallux valgus

IH: instep height

NH: navicular height

IS angle: instep angle

MPH angle: metatarso-phalangeal (mp) -heel angle

TAL: distance of transverse arch

TAH: height of transverse arch

TA: transverse arch

GFH angle: great toe-first metatarsal head-heel angle

SHN angle: second toe-hell-navicular angle

ABD: axis of the bone distance

GSR: great toe-second toe ratio

Declarations

Ethics approval and consent to participate: the study design was approved by the ethical review board at the ryotokuji university (authorization number: 1909). Participants were provided oral and written explanations of the study and publication. All participants signed a consent form prior to the study.

Consent for publication: not applicable

Availability of data and materials: not applicable.

Competing interests: the authors declare that they have no competing interests.

Funding: this work was supported by jsps kakenhi, grant number 18h03559, 18k12161. The funding sources had no involvement in study design; in the collection, analysis and interpretation of data; in the writing of the report; and in the decision to submit the article for publication.

Authors’ contributions: ty and ky planned the study, analyzed the data, and drafted the manuscript. Ty, ky, and ms performed all measurements and contributed to the data acquisition. Ty, ky, ms, tr, mk and sh analyzed all statistical data and contributed to drafting of the manuscript. Tr, yt and sh planned the study, including the instrumentation and contributed to the revision of the manuscript.

Acknowledgements: not applicable.

Authors’ information: not applicable.

References

1. Nix S, Smith M, Vicenzino B. Prevalence of hallux valgus in the general population: a systematic review and meta-analysis. J Foot Ankle Res. 2010;3:21.
2. . Nguyen US, Hillstrom HJ, Li W, Dufour AB, Kiel DP, Procter-Gray E, Gagnon MM, Hannan MT. Factors associated with hallux valgus in a population-based study of older women and men: the MOBILIZE Boston Study. Osteoarthritis Cartilage. 2010;18:41-6.
3. Menz HB, Roddy E, Thomas E, Croft PR. Impact of hallux valgus severity on general and foot-specific health-related quality of life. Arthritis Care Res (Hoboken). 2011;63:396-404.
4. Pedro V. Munuera, Juan Polo, Jesús Rebollo. Length of the first metatarsal and hallux in hallux valgus in the initial stage. Int Orthop. 2008;32:489–495.
5. D'Arcangelo PR, Landorf KB, Munteanu SE, Zammit GV, Menz HB. Radiographic correlates of hallux valgus severity in older people. J Foot Ankle Res. 2010;16;3:20.
6. King DM, Toolan BC. Associated deformities and hypermobility in hallux valgus: an investigation with weightbearing radiographs. Foot Ankle Int. 2004;25:251-255.
7. Roddy E1, Zhang W, Doherty M. Prevalence and associations of hallux valgus in a primary care population. Arthritis Rheum. 2008;59:857-62.
8. Nishimura A, Fukuda A, Nakazora S, Uchida A, Sudo A, Kato K, Yamada T. Prevalence of hallux valgus and risk factors among Japanese community dwellers. J Orthop Sci. 2014 Mar;19(2):257-262.
9. Menz HB, Morris ME. Footwear characteristics and foot problems in older people. Gerontology. 2005;51:346-351.
10. Galica AM, Hagedorn TJ, Dufour AB, Riskowski JL, Hillstrom HJ, Casey VA, Hannan MT. Hallux valgus and plantar pressure loading: the FraminGFH anglem foot study. J Foot Ankle Res. 2013;6:42.
11. Telfer S, Woodburn J. The use of 3D surface scanning for the measurement and assessment of the human foot. J Foot Ankle Res. 2010;3:19.
12. Stanković K, Booth GB, Danckaers F, Burg F, Vermaelen P, Duerinck S, Sijbers J, Huysmans T. Three-dimensional quantitative analysis of healthy foot shape: a proof of concept study. J Foot Ankle Res. 2018;11: 8.
13. Nix SE, Vicenzino BT, Collins NJ, Smith MD. Characteristics of foot structure and footwear associated with hallux valgus: a systematic review. Osteoarthritis Cartilage. 2012;20:1059-1074.
14. Yamashita K, Yamashita T, Sato M, Kawasumi M, Takase Y. Development of a quantitative measurement system for three-dimensional analysis of foot morphology using a smartphone. Conf Proc IEEE Eng Med Biol Soc. 2019.
15. Pique-Vidal C, Vila J. A geometric analysis of hallux valgus: correlation with clinical assessment of severity. J Foot Ankle Res 2009;2:15.
16. Vicenzino B, Griffiths SR, Griffiths LA, Hadley A. Effect of antipronation tape and temporary orthotic on vertical navicular height before and after exercise. J Orthop Sports Phys Ther. 2000;30:333-339.
17. Mueller TAHost JV, Norton BJ. Navicular drop as a composite measure of excessive pronation. J Am Podiatr Med Assoc. 1993;83:198-202.

18. Arangio GA, Salathe EP. A biomechanical analysis of posterior tibial tendon dysfunction, medial displacement calcaneal osteotomy and flexor digitorum longus transfer in adult acquired flat foot. Clin Biomech 2009; 24(4):385-90.
19. Caravaggi P, Sforza C, Leardini A, Portinaro N, Panou A. Effect of plano-valgus foot posture on midfoot kinematics during barefoot walking in an adolescent population. J Foot Ankle Res. 2018;11:55.
20. Lange B, Chipchase L, Evans A. The effect of low-Dye taping on plantar pressures, during gait, in subjects with navicular drop exceeding 10 mm. J Orthop Sports Phys Ther. 2004;34:201-209.
21. Hagedorn TJ, Dufour AB, Riskowski JL, Hillstrom HJ, Menz HB, Casey VA, Hannan MT. Foot disorders, foot posture, and foot function: the Framingham foot study. PLoS One. 2013;8(9):e74364.
22. Friedrich H. W. Heuck, Brigitte R. G. Bast. Radiologische Skizzen und Tabellen. Peripheres Skelett. Stuttgart New York: Thieme; 1994.
23. Woźniacka R, Bac A, Matusik S, Szczygieł E, Ciszek E. Body weight and the medial longitudinal foot arch: high-arched foot, a hidden problem?. Eur J Pediatr. 2013;172(5):683-691.
24. Stavlas P, Grivas TB, Constantinos M, Vasiliadis E, Polyzois V. The evaluation of foot morphology in children between 6 and 17 years of age: a cross-sectional study based on footprints in a Mediterranean population. J Foot Ankle Surg. 2005;44(6):424–428.
25. Watanabe K, Kitaoka HB, Fujii T, Crevoisier X, Berglund LJ, Zhao KD, Kaufman KR, An KN. Posterior tibial tendon dysfunction and flatfoot: analysis with simulated walking. Gait Posture. 2013;37:264-268.
26. Komeda T, Tanaka Y, Takakura Y, Fujii T, Samoto N, Tamai S. Evaluation of the longitudinal arch of the foot with hallux valgus using a newly developed two-dimensional coordinate system. J Orthop Sci. 2001;6:110-118.

Figures

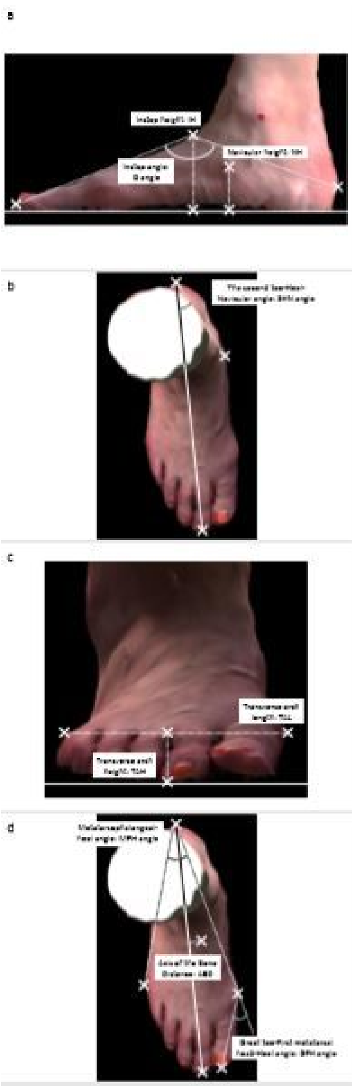

Figure 1

The Foot Skeletal Features